Applied Catalysis B: Environmental 119–120 (2012) 287–296

Contents lists available at SciVerse ScienceDirect

Applied Catalysis B: Environmental

journal homepage: www.elsevier.com/locate/apcatb

In situ investigation of Diesel soot combustion over an $AgMnO_x$ catalyst

N. Guilhaume *, B. Bassou, G. Bergeret, D. Bianchi, F. Bosselet, A. Desmartin-Chomel, B. Jouguet, C. Mirodatos

Université Lyon 1, Institut de recherches sur la catalyse et l'environnement de Lyon IRCELYON, UMR5256 CNRS, 2 avenue Albert Einstein, F-69626 Villeurbanne Cedex, France

ARTICLE INFO

Article history:
Received 2 March 2012
Accepted 6 March 2012
Available online 13 March 2012

Keywords:
Diesel soot
Soot combustion
Mechanism
Ag–Mn mixed oxide
In-situ XRD
Oxygen isotopic exchange

ABSTRACT

An $AgMnO_x$ catalyst (3.5 wt.% Ag) incorporating silver ions in a Mn_2O_3 phase exhibits high performances for soot oxidation below 300 °C. Its structural and redox properties have been investigated under reaction conditions using in situ XRD and DTA-TGA measurements. The catalyst appears unmodified during soot combustion experiments under oxygen, but in the absence of oxygen the soot is stoichiometrically oxidised by lattice oxygen leading to catalyst bulk reduction according to the steps $Mn_2O_3 \rightarrow Mn_3O_4 \rightarrow MnO$.

The isotopic reaction product composition ($C^{16}O_2$, $C^{18}O^{16}O$, $C^{16}O_2$, $C^{16}O$ and $C^{18}O$) obtained during soot combustion experiments under $^{18}O_2$ reveals that the reaction follows a redox mechanism, in which the transfer of lattice oxygen from the catalyst to the soot is responsible for the soot ignition at low temperature.

1. Introduction

The implementation in 2011 of Euro 5 emission standards now restricts the particulate emissions of Diesel passenger cars and light commercial vehicles to 0.005 g/km, which makes the introduction of Diesel particulate filters (DPFs) mandatory. Wall-flow ceramic monoliths ensure a high filtration efficiency of particles (>99% for 20–500 nm particles) based on surface (or "cake") filtration [1]. The particles are trapped in the monolith channels and form a cake on the filter surface, which requires periodic regeneration of the filtration properties by burning the soot. The temperature of Diesel exhaust gases, however, is relatively low (100–450 °C) and does not reach the spontaneous soot ignition temperature (550–600 °C). Consequently, the filter regeneration requires a computer-driven technology that monitors the pressure drop in the filter, continuously delivers a cerium-based additive directly into the fuel (fuel-born catalyst) and periodically increases the DPF temperature by additional fuel combustion in a pre-oxidizer to initiate the regeneration. On top of its high cost, this process presents drawbacks, such as thermal damage due to severe and uncontrolled regeneration cycles [2], and a significant fuel penalty resulting from the additional consumption to heat the filter. In addition, the filter must be cleaned periodically to remove ceria deposits, whereas ceria nanoparticles that could escape the filter might represent an environmental concern if spread in the atmosphere at large scale. Therefore, the development of catalytic filters requires catalysts to be coated within the filter, to avoid the use of additives in the fuel and to promote soot combustion at lower temperatures, ideally below 450 °C to design a continuously regenerating trap.

The reactivity of carbon materials as regards combustion and gasification has been widely investigated, due to its relevance to coal utilization. The reaction mechanisms, however, are complex and difficult to study because they involve both atomic and macroscopic processes, the reactions are highly exothermic and difficult to control. As regards the catalytic oxidation of soot, the catalytic performances are also strongly dependent on the reaction conditions (use of real soot or model carbon, type of contact, particle size, catalyst/soot ratio, heating rate, oxygen partial pressure, presence of NO_x). Moulijn and Kapteijn [3] proposed a unified mechanism for the oxidation of carbon materials, valid for un-catalysed as well as alkali-catalysed reactions, that attempts to describe the reactions of carbon with any oxygen-containing molecule (i.e. CO_2, H_2O, O_2, NO, N_2O). Early studies on the mechanism of catalytic carbon oxidation postulated that metal oxides could catalyse the oxidation of carbon only if their direct reduction by carbon (i.e. "carbothermal reduction") was thermodynamically possible [4]. Since then, however, other mechanisms involving surface oxygen species have been postulated or demonstrated. For some perovskite oxides such as lanthanum chromites, weakly chemisorbed oxygen species have been proposed to be responsible for soot combustion [5,6]. Mul et al. [7] used $^{18}O_2$ to study the mechanism of carbon black oxidation catalysed by several simple transition metal oxides (Cr_2O_3, Co_3O_4, Fe_2O_3, MoO_3, V_2O_5 and K_2MoO_4). They proposed three different possible mechanisms depending on the catalyst:

* Corresponding author. Tel.: +33 0 472 445 389; fax: +33 0 472 445 399.
E-mail address: Nolven.Guilhaume@ircelyon.univ-lyon1.fr (N. Guilhaume).

0926-3373/$ – see front matter © 2012 Elsevier B.V. All rights reserved.
doi:10.1016/j.apcatb.2012.03.009

(i) a surface redox mechanism for Co_3O_4 and Fe_2O_3, (ii) a dual surface redox and spill-over mechanism also involving adsorbed oxygen species for Cr_2O_3, and (iii) a redox mechanism involving lattice oxygen for MoO_3, V_2O_5 and K_2MoO_4. Machida et al. [8] also studied carbon black oxidation under $^{18}O_2$ pulses over ceria-based catalysts, but they could not discriminate between two possible reaction pathways involving either adsorbed superoxide ions or lattice oxygen. Other studies of soot oxidation on La^{3+}-doped ceria [9] or Ag deposited on ceria [10] showed that the lattice oxygen of cerium oxide was involved in the reaction mechanism, the dopants improving the reducibility of ceria. In an experimental microkinetic study of soot oxidation catalysed by ceria [11,12], we could demonstrate that the number of contacts at the ceria/soot interface is a key parameter in the soot oxidation process, and that the catalyst/soot contacts are the maintained during the reaction, in keeping with the observations of Simonsen et al. [13] by environmental transmission microscopy. Recently, however, Yamazaki et al. [14] proposed that weakly adsorbed oxygen species on a CeO_2-Ag catalyst are the active species for soot oxidation.

We have described previously the development of a high throughput screening procedure to evaluate various oxide and mixed oxide catalysts for Diesel soot combustion [15,16]. From these results, Bi, Mn and Ag simple oxides and Bi/Mn and Ag/Mn mixed oxides were identified as particularly active catalysts. Following this primary screening, an optimised formulation was obtained by design of experiments based on the identification of primary metal–metal interactions in a ternary Ag–Mn–Bi system [17,18]. It revealed that bismuth was not an essential component and allowed us to further optimize the Ag/Mn ratio to a weight composition of 3.5% Ag. Although supported Ag catalysts [10,14,19] and Mn oxides [20] have been separately reported to catalyse soot oxidation, Ag-doped Mn oxides have not, up to now, been studied for soot combustion.

In the present study, we present the performances of the optimised Ag–Mn oxide catalyst, which is active for soot oxidation below 300 °C. In situ XRD experiments and DTA-TGA measurements were performed during the catalytic soot oxidation in the presence and in the absence of oxygen, with the objective to gain insight on the effect of silver on the performances and on the role of the redox properties in the catalytic activity. Isotopic oxygen exchange and soot combustion experiments in the presence of $^{18}O_2$ were used to characterize the reactive oxygen species. On the basis of the results presented, a mechanism for soot oxidation over 3.5%$AgMnO_x$ is proposed.

2. Experimental

2.1. Catalyst and soot

The Ag-doped Mn oxide catalyst was synthesised using the citrate-gel method. An aqueous solution of Ag and Mn nitrates (Ag/Mn molar ratio = 2.7%) was mixed with citric acid in the proportion of 1 mol citric acid per mole of nitrate. The pH of the solution was adjusted at 6–7 by addition of concentrated ammonia. This solution was slowly evaporated under stirring at 90 °C, until a viscous gel was formed. The gel was successively heated at 110, 130 and 170 °C in an oven, which leads to gel swelling into a voluminous powder. The powder was grinded in a mortar and finally calcined at 600 °C in flowing air for 3 h (fresh catalyst).

Hydrothermal ageing was performed by calcining the fresh catalyst at 750 °C in a flow of air containing 4 vol.% of steam for 21 h (aged catalyst).

The soot samples were collected in a flow-through particle trap placed in the exhaust stream of a 2.2L Renault Diesel engine after an oxidation catalyst, therefore minimizing the content of adsorbed hydrocarbons. Additionally, the soot samples were calcined at 400 °C in air to remove weakly adsorbed species.

2.2. Characterisation

Specific surface areas were measured by nitrogen adsorption on an ASAP 2010 equipment. The samples were previously desorbed under 10^{-5} mbar at 300 °C for 1 h.

Chemical analyses of Ag were performed by inductively coupled plasma (ICP). The soot chemical composition was determined using a CHNS-O analyser.

X-ray powder patterns of samples were collected using two instruments (Cu Kα radiation 0.154184 nm, diffracted beam graphite monochromator). For standard measurements at room temperature under air, the data were collected using a Bruker D5005 diffractometer equipped with a scintillation detector. In-situ measurements were carried out using a Panalytical X'Pert Pro MPD diffractometer (Bragg–Brentano para-focusing geometry, reflection mode) equipped with a 1-dimensional multistrip detector (X'Celerator, 127 channels on 2.1°). The samples were mounted in an atmosphere-controlled Anton Paar XRX 900 reactor chamber. The temperature-regulated glass-ceramic sample holder was open to allow the gas to flow through the sample (N_2 or synthetic air). Heating was performed by steps up to 600 °C at a rate of 2 °C/min. The diffractograms were collected under isothermal conditions (0.0334° (2θ) and 512 s/step, 97 min per scan), after a stabilisation time of 1 h between each temperature modification.

Phase identification was performed using the DiffracPlus Eva software (Bruker) and the ICDD-PDF4+ database. The quantitative phase amounts were determined by the Rietveld method (Fullprof code, full program and documentation can be obtained at http://www.ill.eu/sites/fullprof).

X-ray photoelectron (XPS) and Auger Spectra were recorded using an Axis Ultra DLD spectrometer (Kratos Analytical).

Thermal analyses (DTA-TGA) were performed in air with a SETARAM analyser equipped with a mass spectrometer for outlet gas analysis. The samples were placed in a Pt crucible and heated at 5 °C/min under a flow (50 mL/min) of synthetic air or pure N_2. The gases desorbing during the temperature ramps were monitored with a mass spectrometer.

2.3. Catalytic tests

Two types of contacts for the catalyst/soot mixture were used in the catalytic experiments. The tight contact was achieved by grinding a catalyst/soot mixture (90 wt./10 wt. ratio) in an agate mortar for 5 min. For loose contact conditions, the catalyst and soot were simply mixed with a spatula. We observed previously that tight contact is more appropriate to accurately evaluate the catalytic performances because the soot/catalyst mixture is more homogeneous than in loose contact [11,12,15]. The loose contact, however, is more representative of a washcoated DPF [21,22].

Catalytic tests were performed in a fixed bed quartz microreactor equipped with a thermocouple inserted in the catalyst/soot bed to monitors its temperature T_s independently of the oven temperature. The catalytic bed consisted in 360 mg catalyst + 40 mg soot, in order to provide enough volume to insert the thermocouple into the packed bed. The catalyst/soot mixture was heated linearly at 5 °C/min from 25 to 600 °C under a 40 mL/min gas flow (50% O_2 in Ar). The soot ignition temperature T_{ign} corresponding to the light-off process was defined as the intersection between two tangents on the to the $T_s = f(t)$ profile, as described previously [15,16] (see Fig. 3A). The experimental error on the determination of soot ignition temperature was estimated at ±3 °C. The gaseous products stream at the reactor outlet was analysed with a mass spectrometer.

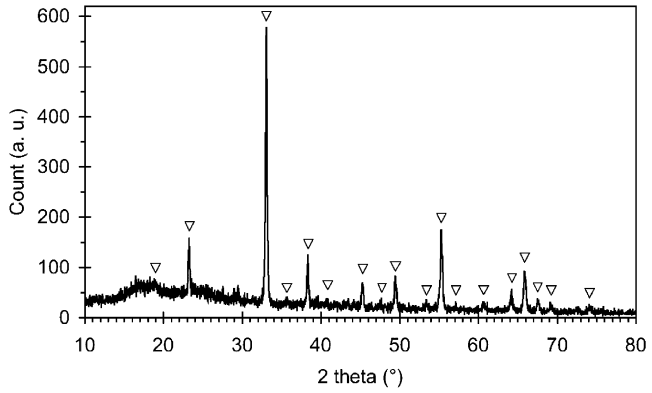

Fig. 1. XRD pattern of the 3.5 wt.%$AgMnO_x$ catalyst calcined at 600 °C. The triangles correspond to the diffraction lines of Mn_2O_3 (bixbyite, ICDD-PDF file 00-041-1442).

2.4. Isotopic oxygen exchange and soot combustion experiments using $^{18}O_2$

Isotopic exchange experiments using $^{18}O_2$ were performed with a gas flow setup equipped with two independent gas-feed streams and a four-port automated valve to switch between unlabelled and labelled gas streams. Catalyst and catalyst/soot samples were placed in a quartz micro-reactor between two quartz wool plugs. The reactor was tapered at the outlet and the inlet dead volume was filled with quartz powder (200–300 μm) to minimize the dead volumes. For isotopic oxygen switch without reaction, a mixture of 20% $^{16}O_2$ in argon (total flow rate 50 mL/min) was passed over the catalyst (40 mg) and allowed to stabilize. After steady mass spectrometer signals were obtained, the flow was switched to that containing 20% $^{18}O_2$ and 10% He in argon, and the exchange was carried out at 300 and 400 °C. For light-off experiments in the presence of labelled oxygen, the first gas mixture contained 33% $^{16}O_2$ in argon, and the second mixture contained 33% $^{18}O_2$, 7% He and 60% Ar, with a total flow rate of 60 mL/min. The reactor containing the catalyst/soot sample (56 mg, catalyst:soot mass ratio of 90:10, tight contact) was heated at 5 °C/min under $^{16}O_2$ in Ar up to 220 °C, i.e. before the soot ignition takes place, then the gas mixture was switched to that containing $^{18}O_2$ and heating was continued up to 300 °C, at which the soot combustion was completed. The relevant m/e fragments corresponding to He, H_2O, CO, $C^{18}O$, $^{16}O_2$, $^{18}O^{16}O$, $^{18}O_2$, Ar, CO_2, $C^{18}O^{16}O$, $C^{18}O_2$ were monitored by a mass spectrometer. The normalised concentration of each isotope for a given species was calculated by dividing the signal for that isotope by the sum of the signals for all the isotopes of that species. The $^{18}O^{16}O$ signal was corrected for the contribution of about 2.5% of $^{18}O^{16}O$ present as impurity in $^{18}O_2$. CO formation was calculated from mass 28 after signal correction for the fragmentation of CO_2 and $C^{18}O^{16}O$, whereas the contribution of residual nitrogen to mass 28 was considered negligible. $C^{18}O$ was deduced from mass 30 after correction for the fragmentation of $C^{18}O_2$ and $C^{18}O^{16}O$.

3. Results

3.1. Catalyst characterisation and thermal stability

The XRD pattern of catalyst calcined at 600 °C (Fig. 1) reveals the presence only of a Mn_2O_3 (bixbyite) phase. No other crystallised phase is detected, but it should be mentioned that the three main reflections of crystalline Ag_2O appear at similar positions as Mn_2O_3 lines. Bulk Ag_2O, however, is thermally unstable and decomposes at 230 °C [23] or even lower temperatures (195 °C according to [24]), therefore its presence can be considered unlikely. This suggests that Ag is present either as well dispersed AgO on Mn_2O_3, or incorporated into the Mn_2O_3 phase as a mixed Ag–Mn oxide.

Chemical analysis confirmed the 3.5 wt.% Ag loading in the solid. XPS analysis of the catalyst gives a binding energy of the Ag $3d_{5/2}$ peak at approximately 368.2 eV, but this does not allow an unambiguous identification of Ag^{2+}, Ag^+ or Ag^0 since the three oxidation states display very close binding energies [25]. Alternatively, the Auger peaks of silver are more sensitive to the chemical environment and can be used in conjunction with the Auger parameter (α), defined as the sum of the kinetic energy of the strongest Auger line (AgM_5VV) and the binding energy of the strongest photoelectron peak (Ag $3d_{5/2}$), to determine whether the oxidised or metallic state is predominant. The Ag M_5NN peak in the fresh catalyst is found at 350.5 eV, which corresponds to an Auger parameter of 718.7 eV. This might correspond either to Ag^{2+} or Ag^+, but not to metallic silver since the α parameter would be close to 726 eV [26,27]. Therefore, the presence of metallic silver in the fresh catalyst can be ruled out.

The specific surface area of the fresh catalyst (calcined at 600 °C) is 19 $m^2\,g^{-1}$, which is the range classically obtained for oxides prepared by the citrates gel method. After hydrothermal ageing at 750 °C in the presence of steam, the surface area is reduced to 12 $m^2\,g^{-1}$.

The thermal stability has been studied by DTA-TGA. Fig. 2 depicts the TG profiles obtained when the catalyst was heated up to 700 °C

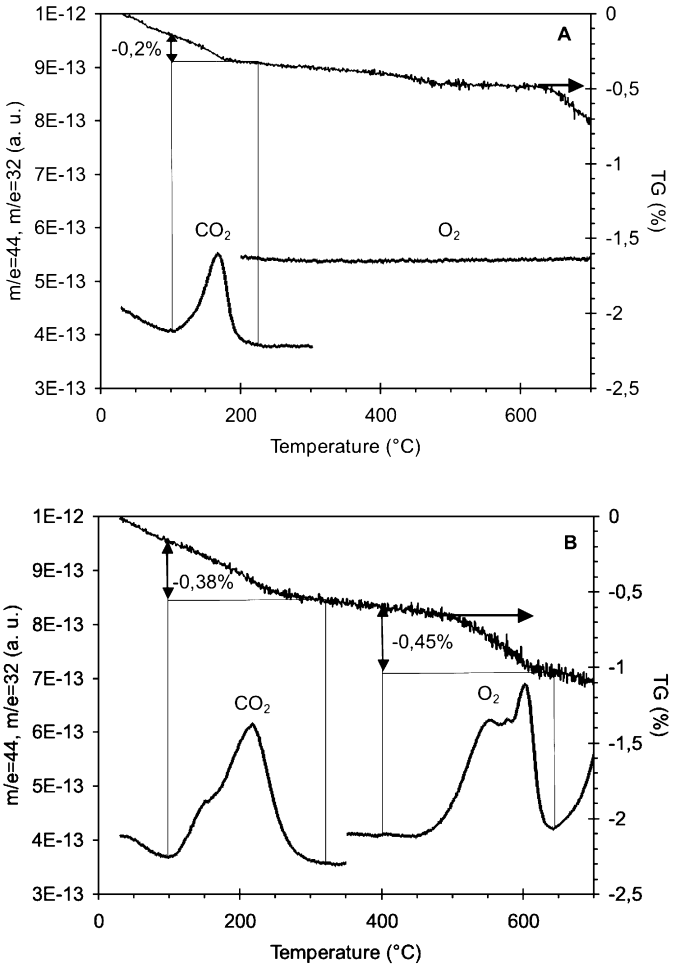

Fig. 2. TGA profiles of 3.5 wt.%$AgMnO_x$ catalyst performed under (A) air (sample mass 20 mg) or (B) nitrogen (sample mass 21 mg) with simultaneous mass spectrometer analysis of O_2 and CO_2.

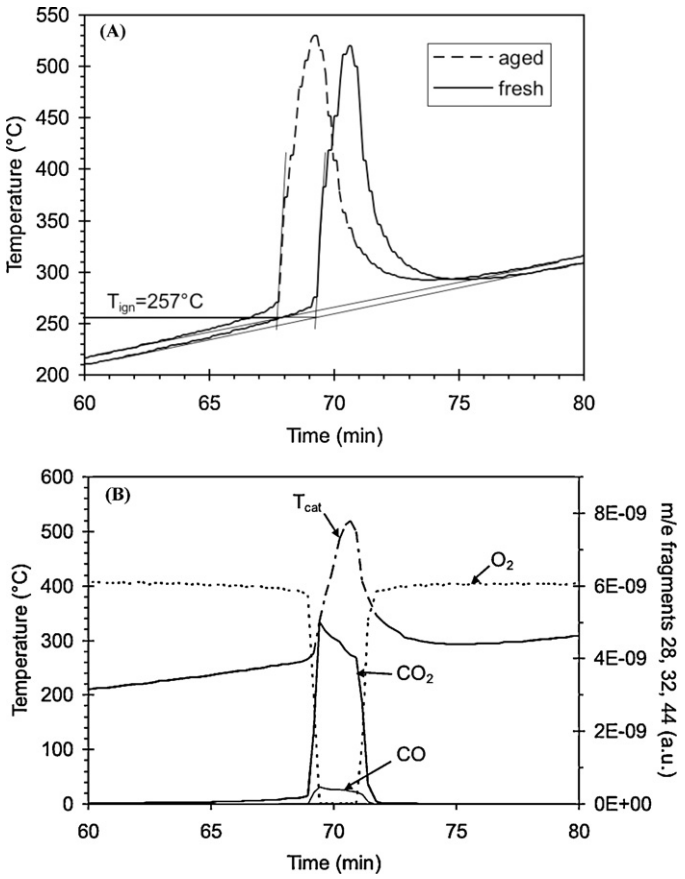

Fig. 3. (A) Onset temperatures of soot combustion process for fresh and aged 3.5 wt.%$AgMnO_x$ catalysts, (B) online analysis of gaseous product stream (fresh catalyst). Conditions: 400 mg catalyst + 40 mg soot in tight contact, heating rate 5 °C/min, 50% O_2 in Ar, total gas flow rate 40 mL/min.

under air or nitrogen. The heat flow profiles are not shown since they exhibit no significant variations. Under air (Fig. 2A), a small mass loss (0.2%) is observed in the 100–200 °C temperature range, which corresponds to the decomposition of surface carbonates, as evidenced by a small CO_2 production peak. Between 200 and 700 °C, an additional mass loss of 0.5% takes place, slowly up to 640 °C, then more rapidly in the 640–700 °C temperature range. This is probably related to the dehydroxylation of the oxide, since a weak variation in the m/e = 18 fragment intensity is observed (not shown), while the O_2 and CO_2 signals do not change. In addition, the thermal profile remains essentially flat up to 700 °C, which reveals the absence of any solid decomposition or phase transition. The final mass loss at 700 °C is 0.7 wt.%. The catalyst appears therefore very stable up to 700 °C.

Under nitrogen (Fig. 2B), CO_2 evolution is also observed in a slightly broader temperature range (100–250 °C, mass loss 0.38%). Between 450 and 645 °C, a second mass loss (0.45%) takes place with simultaneous O_2 appearance following a complex profile. This peak is consistent with the theoretical mass loss (≈0.5 wt.%) associated to the decomposition of AgO according to: $AgO \rightarrow Ag^0 + 1/2O_2$. For comparison, the decomposition of Mn_2O_3 into Mn_3O_4 (first reduction step of Mn_2O_3 [28]) would lead to a 3.4 wt.% mass loss. The amount of O_2 desorbed (232 μmol g^{-1}) also correlates very well with the amount of Ag in the catalyst (463 μmol g^{-1}) and with an O/Ag atomic ratio of 1. The complex oxygen desorption profile might be related to an intermediate decomposition step into Ag_2O, or to the involvement of different Ag^{2+} species such as AgO dispersed on Mn_2O_3 and a mixed $AgMnO_x$ oxide phase. An interesting point is that there is apparently no decomposition of silver oxide up to 700 °C under an air flow, as shown by the O_2 trace in Fig. 2A. This suggests the presence of a strongly stabilised Ag^{2+} species in a mixed oxide phase, since the thermal decomposition in air of bulk AgO powder into metallic silver has been reported to be fully completed at 400 °C [24]. Under nitrogen, however, this silver oxide phase is less stable and starts to decompose at 450 °C.

3.2. Catalytic performance of fresh and aged 3.5%$AgMnO_x$ catalyst for Diesel soot combustion

Soot combustion is a highly exothermic reaction (enthalpy of carbon combustion: −406.4 kJ/mol), and therefore the catalyst resistance to thermal ageing is a prerequisite for any industrial application. The 3.5%$AgMnO_x$ catalyst was therefore evaluated in fresh state (after calcination at 600 °C in air), but also after hydrothermal ageing at 750 °C in the presence of 4 vol.% steam, which promotes the sintering of oxides [29–31].

The evolution of T_s with time on stream during the combustion of soot in tight contact with fresh and aged 3.5%$AgMnO_x$ catalyst is shown in Fig. 3A. The timescale is a little shifted in the two experiments because the initial delay before the oven heating starts is slightly different, but the oven temperature ramps are then strictly identical (5 °C/min). The soot ignition temperatures (measured when the catalyst/soot temperature starts to deviate from the linear oven temperature) are clearly similar for fresh and aged catalysts (T_{ign} = 257 °C). This reveals that the ageing treatment does not impair the catalytic performances in spite of the 37% decrease in the surface area after hydrothermal ageing.

Un-promoted Mn_2O_3 has been tested previously under similar reaction conditions and displayed a light-off temperature of 340 °C [15]. Silver addition in the form of a mixed AgMn oxide in a Ag/Mn atomic ratio of 2.7% appears therefore very efficient to decrease the soot ignition temperature.

The exothermic peak matches the CO_2 production analysed by online mass spectrometry (Fig. 3B). Once initiated, the soot combustion process is very fast and becomes rapidly limited by the molar flow rate of oxygen, since during about 120 s the oxygen is fully depleted. The exothermic peak would probably be stronger and thinner with a higher oxygen flow rate. In addition to the main production of CO_2, a trace amount of CO is formed (Fig. 3B) that might result from incomplete combustion due to transient oxygen under-stoichiometry.

It should be mentioned that the catalyst synthesis was reproduced and that a similar soot ignition temperature was obtained with the second catalyst batch (T_{ign} = 255 °C). The fresh catalyst was also tested in loose contact conditions. The experiments, however, were irreproducible as regards the soot ignition temperature, which was sometimes observed at a similar temperature than in tight contact, but sometimes could not be determined because of a broad and nearly flat $T_s = f(t)$ profile. This is probably related to the inhomogeneity of the catalyst/soot mixture in loose contact [15].

3.3. In-situ DTA-TGA studies: effect of catalyst/soot contact

3.3.1. Soot combustion under oxygen

In order to gain more insight into the effect of contact, in-situ DTA-TGA experiments were performed with soot/catalyst mixtures (10 wt.% soot) in tight or loose contact, and compared with the combustion of pure soot. The results are depicted in Fig. 4. The heat fluxes measured by DTA are all exothermic peaks corresponding to the soot combustion process (Fig. 4A). In the absence of catalyst, the soot burns between 480 and 660 °C, with a maximum rate at about 620 °C. The heat flux matches very closely the CO_2 formation profile shown in Fig. 4B. The final sample mass loss at 700 °C is close to 97%, which means that most of the soot has burned at this temperature. The unburned mass probably corresponds to ashes

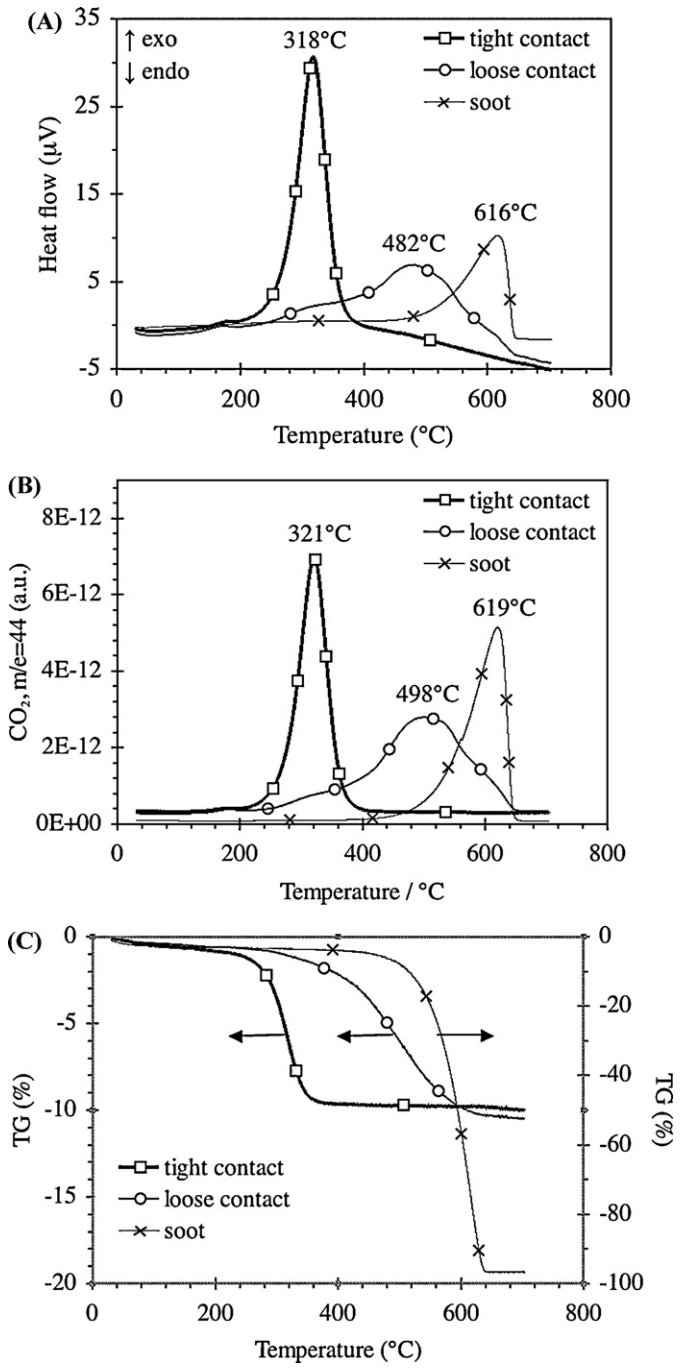

Fig. 4. DTA-TGA analysis of soot combustion in air depending on the type of contact (no catalyst, tight or loose contact with 3.5 wt.%$AgMnO_x$ catalyst). (A) Heat flow profiles (data referred to 1 mg soot); (B) CO_2 analysed at the reactor outlet (data referred to 1 mg soot); (C) TG profiles. Conditions: 10 wt.% soot + 90 wt.% $AgMnO_x$ catalyst in tight contact (10.57 mg sample) or loose contact (9.91 mg sample), or pure soot (3.97 mg sample), heating rate 5 °C/min, air flow rate 50 mL/min.

originating from the engine lubricating oil. This is consistent with the chemical composition of the soot, which is made up of 90.6% C, 0.6% H and 6.3% O (accuracy ±0.2%), with no sulphur or nitrogen detected.

In tight contact, the soot combustion takes place between 220 and 380 °C (maximum at 318 °C) and exhibits more intense heat flux and CO_2 profiles than the pure soot (Fig. 4A and B). The final mass loss reaches ≈10% (Fig. 4C), in agreement with the total combustion of the soot initially present in the mixture. As seen previously, the mass loss of pure 3.5%$AgMnO_x$ catalyst in air at 700 °C is only 0.7% (Fig. 2A). In contrast, the loose soot/catalyst contact leads to a very broad exothermic peak with a maximum at 482 °C, while CO_2 formation takes place in the whole temperature range (240–660 °C) corresponding to both tight contact and pure soot. The loose contact appears to cover all types of catalyst/soot physical contacts, from tight contact to the lack of contact. The final mass loss at 700 °C is again close to 10%, which corresponds to the initial amount of soot in the mixture. It should be mentioned that the areas under the three CO_2 curves shown in Fig. 4B, after correcting the CO_2 signals for the different soot mass, are similar within an error of 8%.

Despite the similar heating rate, soot/catalyst ratio and contact (tight contact), the soot combustion in DTA-TGA experiments is much slower than in micro-reactor (compare Fig. 3B and Fig. 4B): there is no ignition during DTA-TGA but a slow combustion for about 30 min, whereas the sharp ignition burns the soot in 3 min in micro-reactor. This is related to the very different sample loadings (10 mg in DTA-TGA experiments, 400 mg in micro-reactor) and gas flow rates, whereas in DTA-TGA the heat of soot combustion is essentially transferred to the Pt crucible, which prevents the ignition process. However, the exothermic heat flow measured by DTA starts at lower temperature (≈220 °C) than the temperature rise observed in micro-reactor, due to the higher accuracy of the heat flux measurement by DTA.

3.3.2. Soot oxidation in the absence of oxygen

The DTA-TGA experiments were also performed in the absence of oxygen, in order to investigate the oxygen transfers from the 3.5%$AgMnO_x$ catalyst to the soot. The soot alone does not exhibit significant endothermic or exothermic heat fluxes (Fig. 5A), and neither does it burn, as shown by the flat CO_2 profile (Fig. 5B). A progressive mass loss reaching 14% at 700 °C is observed, however (Fig. 5C), whereas MS analysis does not reveal any significant formation of CO_2, H_2O, H_2. This mass loss might be related to the slow decomposition of surface oxygenated complexes into CO (not detected because the experiment is performed under N_2) and to graphitisation of polyaromatic amorphous carbon compounds, as suggested by the two different slopes in the TG profile.

The soot/catalyst mixture in tight contact presents an exothermic peak with a maximum at 441 °C, followed by an endothermic peak with a maximum at 593 °C (Fig. 5A). These peaks matching two intense CO_2 production peaks (Fig. 5B) and mass losses (Fig. 5C) in the same temperature ranges (300–490 °C for the first CO_2 peak, 490–700 °C for the second one). There is also a weak CO_2 peak at 260 °C, appearing as a shoulder to the peak at 215 °C related to surface carbonate desorption from $AgMnO_x$, which might correspond to the reduction of Ag^{2+} induced by oxygen transfer to the soot (see close-up inserted in Fig. 5B). According to previous studies on pure and supported manganese oxides [32–34], the reduction of Mn_2O_3 occurs through the steps:

$$Mn_2O_3 \rightarrow Mn_3O_4 \rightarrow MnO \quad (1)$$

Therefore, the CO_2 peaks can be attributed to soot oxidation by oxygen supplied by the catalyst according to the stoichiometric reactions:

$$260\,^{\circ}C: \quad 2AgO + C \rightarrow Ag + CO_2 \quad (2)$$

$$444\,^{\circ}C: \quad 6Mn_2O_3 + C \rightarrow 4Mn_3O_4 + CO_2 \quad (3)$$

$$594\,^{\circ}C: \quad 4Mn_3O_4 + 2C \rightarrow 12MnO + 2CO_2 \quad (4)$$

This is consistent with the temperature range reported for the reduction steps of manganese oxides, and with the fact that the area of the CO_2 peak at 594 °C is twice that of the peak at 444 °C.

Despite the heat provided by soot combustion, the CO_2 production at 594 °C appears as an endothermic peak. This is due to the

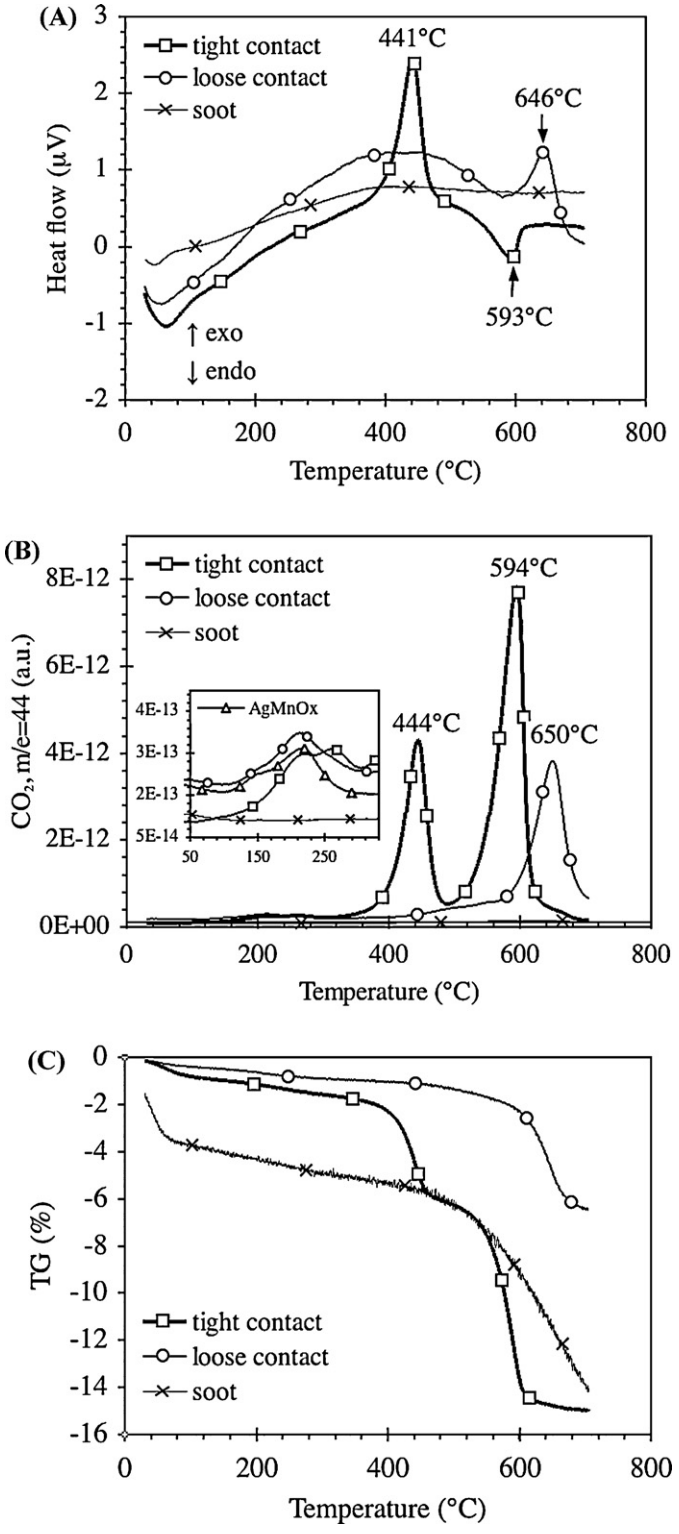

Fig. 5. DTA-TGA analysis of soot combustion under N2 and different contact types (no catalyst, tight or loose contact with 3.5 wt.%$AgMnO_x$ catalyst). (A) Heat flow profiles (data referred to 1 mg soot); (B) CO_2 analysed at the reactor outlet (data referred to 1 mg soot); (C) TG profiles. Conditions: 10 wt.% soot + 90 wt.%$AgMnO_x$ catalyst in tight contact (35.08 mg sample) or loose contact (17.40 mg sample), or pure soot (3.82 mg sample), heating rate 5 °C/min, 50 mL/min N_2.

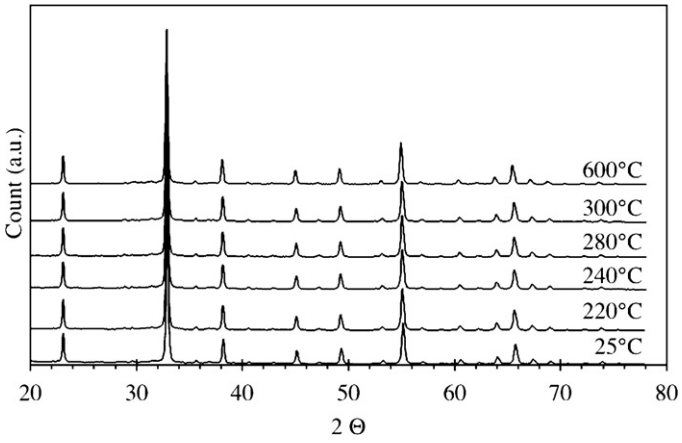

Fig. 6. In situ X-ray diffractograms of soot/3.5 wt.%$AgMnO_x$ mixtures (10 wt.% soot) in tight contact vs. temperature, under O_2/N_2. Conditions: 157 mg soot/catalyst mixture, 50% O_2/50% N_2, total gas flow rate 23 mL/min.

fact that Mn_3O_4 decomposition into MnO is an endothermic process that overlaps the heat produced by the soot oxidation. The final mass loss at 700 °C reaches 15%, from which about 2% correspond to an initial desorption of water and surface carbonates between room temperature and 220 °C. The theoretical total mass loss associated to the complete reduction of AgO and Mn_2O_3 into Ag and MnO is 9.2%. The amount of oxygen supplied by these reactions represents only 35% of the stoichiometric amount required to oxidize the soot into CO_2 (assuming that the soot consists only of carbon), which should correspond to a mass loss of 3.5%. The total mass loss expected from catalyst reduction and soot oxidation is 12.7%, which is consistent with the experimental data (13%).

For the catalyst/soot mixture in loose contact, only one exothermic peak is observed at ≈650 °C, associated to CO_2 production and to a mass loss of ≈4.5%. The CO_2 and TG profiles are actually very similar to the first part of the same profiles in tight contact, but shifted by +200 °C.

3.4. In-situ X-ray diffraction studies

In-situ XRD was used to evaluate the catalyst structure modifications and stability during the soot oxidation reactions in the presence and in the absence of oxygen.

3.4.1. Soot oxidation under oxygen

Fig. 6 depicts the diffraction patterns of soot/catalyst mixtures in tight contact at different temperature under oxygen. At room temperature, the powder displays only the characteristic lines of the Mn_2O_3 phase. The soot itself is essentially amorphous, with only one thin reflection at 26.8° (2θ) characteristic of a crystalline graphite structure [15,35], but this line is not observed in Fig. 6 because there is only 10 wt.% soot in the mixture and this line is weak compared to the pattern of Mn_2O_3. Upon heating at different temperatures up to 600 °C in the presence of oxygen, the patterns are not modified, which means that the soot combustion does not modify irreversibly the catalyst structure, at least considering the time scale of XRD measurements which require 97 min for each diffractogram collection. In other terms, any fast and reversible structure change occurring for instance during the soot ignition will not be detected by this in-situ XRD monitoring.

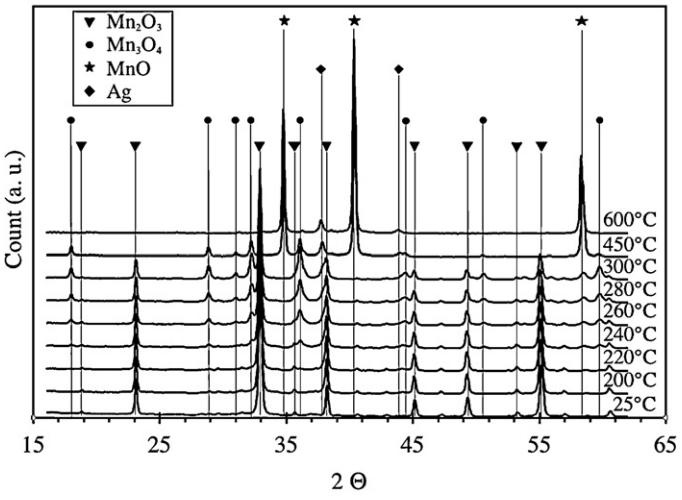

Fig. 7. In situ X-ray diffractograms of soot/3.5 wt.%$AgMnO_x$ mixtures (10 wt.% soot) in tight contact vs. temperature, under N_2. Conditions: 150 mg soot/catalyst mixture, 20 mL/min N_2.

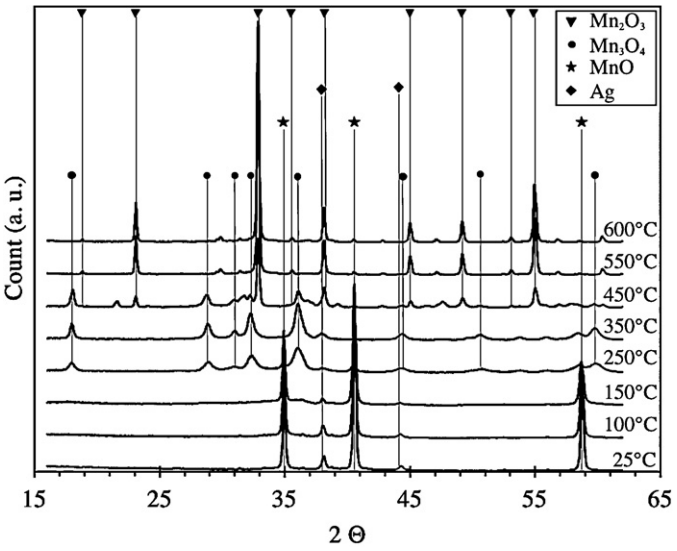

Fig. 8. In situ X-ray diffractograms of the reoxidation in air of $AgMnO_x$ after soot oxidation in the absence of oxygen. Conditions: 38 mL/min air.

3.4.2. Soot oxidation in the absence of oxygen

Fig. 7 shows the evolution of the soot/catalyst diffraction patterns between 25 and 600 °C under nitrogen. Between 200 and 220 °C (the diffractogram recorded at 200 °C is not shown for clarity), the only phase detected is Mn_2O_3, but at 240 °C the main reflections of Mn_3O_4 appear. From 240 °C up to 300 °C, the Mn_3O_4 phase appears and grows at the expense of Mn_2O_3, whereas the main reflection of metallic silver at ≈38° appears as the shoulder of an Mn_2O_3 line. Phase quantification using the Rietveld method (Table 1) shows that the Mn_2O_3 and Mn_3O_4 phases are present at an approximately equivalent ratio at 300 °C. At 450 °C, Mn_2O_3 has completely disappeared, which clearly reveals the presence of metallic silver. MnO is now the main phase (≈80%), whereas about 20% Mn_3O_4 is still present. At 600 °C, only MnO remains and the two most intense lines of Ag^0 are now clearly seen. It should be mentioned that with the catalyst/soot mass ratio of 10 used in all experiments, the soot is in excess with respect to its stoichiometric reaction with the catalyst lattice oxygen. As previously stated, the total reduction of Ag^{2+} (into Ag^0) and Mn^{3+} (into Mn^{2+}) supplies only 35% of the stoichiometric amount of oxygen required to oxidize the soot into CO_2, assuming that the soot is composed of carbon. Consequently, these experiments reveal the progressive catalyst reduction by an excess of soot. The reduction steps of Mn_2O_3 are observed in slightly different temperature ranges than the CO_2 peaks in DGA-TGA experiments (Fig. 5B) because the temperature conditions are different: isothermal conditions for in-situ XRD vs. heat ramp (5 °C/min) in DTA-TGA. The phase transformations revealed by XRD confirm, however, the soot/catalyst reactions in Eqs. (2)–(4).

Table 1
Quantitative Mn oxide phase analysis using Rietveld refinement of the powder diffraction patterns during soot oxidation at different temperatures in the absence of oxygen. Values are given in percent ±2.

T (°C)	Mn_2O_3	Mn_3O_4	MnO
25	100	0	0
200	100	0	0
220	98	2	0
240	87	13	0
260	76	24	0
280	66	34	0
300	51	49	0
450	0	18	82
600	0	0	100

3.4.3. Catalyst reoxidation

The catalyst reoxidation under air following reaction with soot in the absence of oxygen was also monitored by in situ XRD at different temperatures (Fig. 8). Initially, the catalyst is reduced and consists of MnO and metallic silver. At 100 °C, the reflections of Ag^0 begin to weaken, due to amorphisation of the silver particles. At 150 °C, the reflections of MnO start to decrease while those of Mn_3O_4 appear, their proportion reversing progressively up to 350 °C. At 350 °C, no more MnO remains and Mn_3O_4 is now the main phase present, simultaneously with two weak lines that might be attributed to an Mn_5O_8 phase (at 21.7 and 47.8° 2θ). At 450 °C, Mn_3O_4 decreases, Mn_5O_8 increases and the reflections of Mn_2O_3 appear. At 550 °C and 600 °C, Mn_3O_4 and Mn_5O_8 have disappeared and Mn_2O_3 is essentially identified. No silver phase (as metallic or oxide phase) is observed between 250 and 600 °C. These experiments show that: (i) the initial reoxidation of MnO into Mn_3O_4 is rapid since it starts at 150 °C, but the full reoxidation into Mn_2O_3 requires temperatures >450 °C, and (ii) metallic silver appears to be fully reoxidised between 250 and 600 °C, but essentially as an amorphous phase.

3.5. Isotopic oxygen exchange experiments and soot combustion using $^{18}O_2$

The nature of oxygen species involved in the soot combustion was investigated using labelled oxygen. The oxygen exchange capacity of the 3.5%$AgMnO_x$ catalyst was first evaluated in isotopic exchange experiments using $^{18}O_2$.

Fig. 9 shows an oxygen exchange experiment over 3.5%$AgMnO_x$ at 300 °C, which corresponds to the soot ignition temperature in tight contact with the catalyst. Upon switching to labelled oxygen, the $^{18}O_2$ signal follows closely that of the He tracer, suggesting the absence of oxygen exchange. Only a very small amount of cross-labelled $^{18}O^{16}O$ is formed over the catalyst, which confirms that the gas phase oxygen exchange is very limited at this temperature. Similar results were obtained at 400 °C.

A soot combustion experiment performed under $^{18}O_2$ at a heating rate of 5 °C/min is shown in Fig. 10. Unlabelled oxygen was switched to $^{18}O_2$ when the catalyst/soot mixture reached 220 °C and when the light-off starts at ≈270 °C, $^{16}O_2$ has been completely flushed by $^{18}O_2$. Unlabelled $C^{16}O_2$ (Fig. 10A) is the most abundant species formed when the soot ignition begins, followed by smaller

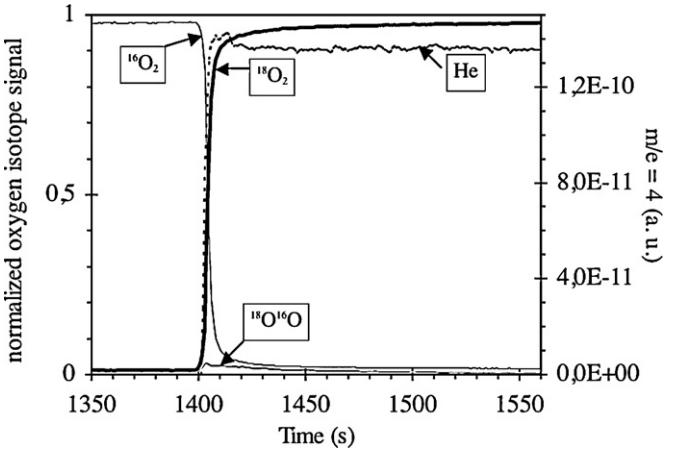

Fig. 9. Normalised oxygen-exchange transients over $AgMnO_x$ at 300 °C. Conditions: 40 mg catalyst, total flow 50 mL/min, step 1: 20% $^{16}O_2$ in argon, step 2: 20% $^{18}O_2$ and 10% He in argon.

amounts of $C^{18}O^{16}O$, while $^{18}O_2$ is nearly fully consumed simultaneously (Fig. 10C). When the $C^{16}O_2$ signal falls off, the $C^{18}O_2$ signal starts to increase, while the $C^{18}O^{16}O$ signal tails off to a relatively high level. During this second part of the soot combustion process ($t \geq 3114$ s), it can be noticed in Fig. 10C that $^{18}O^{16}O$ and to a lower extent $^{16}O_2$ are produced, until the $^{18}O_2$ consumption ends. Unlabelled CO (Fig. 10B) is also produced in trace amount, but no $C^{18}O$ is detected. Since the only source of ^{16}O is the oxygen atoms of the catalyst, these results provide clear evidence as to the involvement of lattice oxygen at the onset of the soot ignition process.

4. Discussion

Catalytic soot oxidation requires oxygen transfer from the catalyst to the soot to initiate the soot combustion at low temperature, and therefore a direct or at least close contact is necessary, except for specific low melting point catalysts that form volatile active species [1]. This has been elegantly demonstrated by the work of Simonsen et al. [13] using environmental TEM and a ceria catalyst: the authors showed that the catalytic oxidation takes place at the soot–CeO_2 interface and that this contact is maintained in the course of the oxidation process. The same conclusion was drawn from our previous studies on the combustion of ceria/soot mixtures using an experimental microkinetic approach [11,12].

Various forms of oxygen exist on the surface of metal oxides. Gaseous oxygen incorporation into the solid as lattice oxygen proceeds by electron transfer according to the general scheme [36]:

$$O_{2(g)} \rightarrow O_{2(ads)} \rightarrow {O_2}^-_{(ads)} \rightarrow {O_2}^{2-}_{(ads)} \rightarrow {O}^-_{(ads)} \rightarrow {O}^{2-}_{(ads)} \rightarrow {O}^{2-}_{(lattice)}$$

Some of these species react with alkanes and alkenes to give partial or total oxidation products, and the selectivity towards oxidation products is strongly related to the nature and concentration of the reactive species [37,38]. Oxygen species adsorbed on manganese oxides have not been much investigated, but superoxide ions ${O_2}^-$ have been identified on MnO–MgO solid solutions [37], whereas ${O_2}^-$ or ${O}^-$ ions have been suggested as active oxygen species for the oxidation of carbon monoxide on MnO_2 [39]. Surface oxygen species weakly adsorbed on lanthanum chromite perovskite catalysts have also been proposed to be responsible for soot combustion by spillover at 300–500 °C [5], as also shown recently with a CeO_2-Ag catalyst [14].

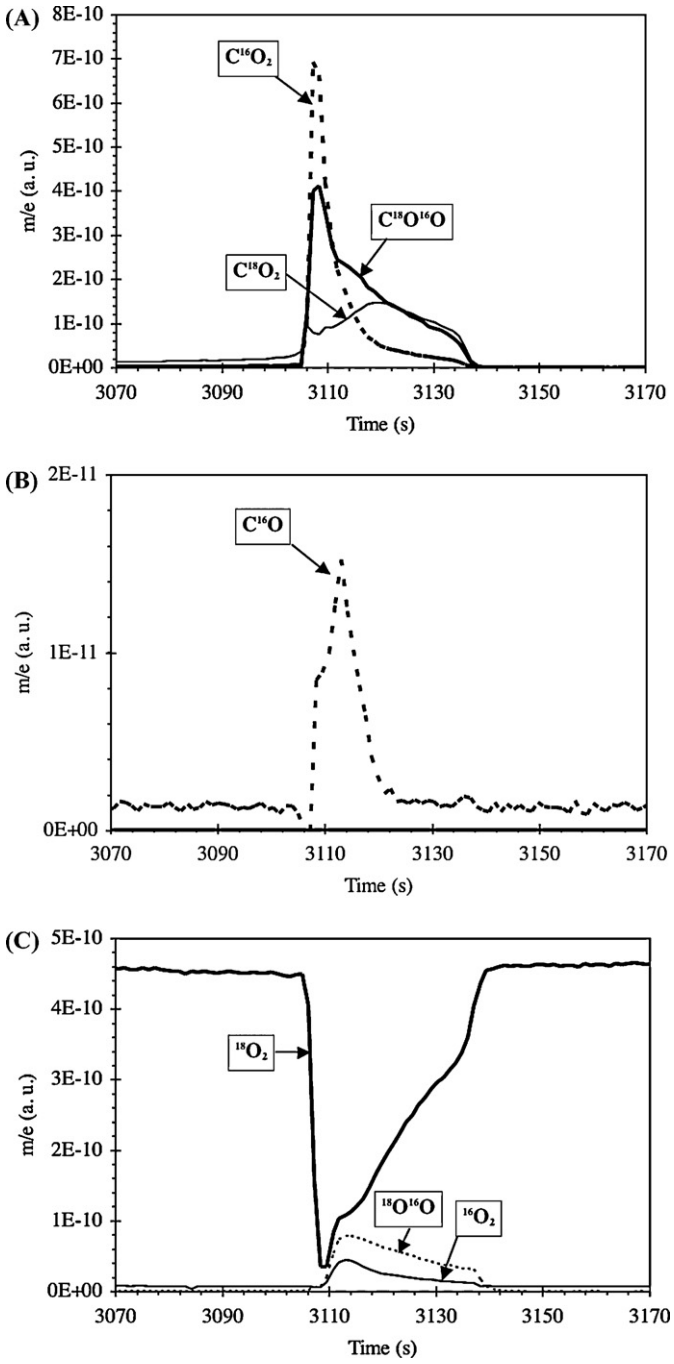

Fig. 10. Soot/$AgMnO_x$ combustion experiment under $^{18}O_2$. (A) CO_2 isotope profiles, (B) CO isotope profiles; (C) O_2 isotope profiles. Conditions: 10 wt.% soot + 90 wt.% $AgMnO_x$ catalyst in tight contact (56.6 mg sample), 33% O_2 and 7% He in Ar (total flow rate 60 mL/min), heating rate 5 °C/min.

4.1. Catalytic performances and structural modifications during soot combustion

The 3.5%$AgMnO_x$ catalyst exhibits very good performances for soot oxidation below 300 °C. The soot ignition temperature is about 80 °C lower over Ag-doped manganese oxide compared to pure Mn_2O_3, which suggests that the role of silver might be to promote oxygen transfer from the catalyst to the soot. Imamura et al. [40] also mentioned a synergetic effect between silver and manganese for CO oxidation catalysed by a Mn–Ag composite oxide. They observed that Ag was stabilised in an oxidised state by the presence of Mn_2O_3, which provided oxygen to silver by reduction.

The reoxidation of reduced Mn was rapid in comparison with that of metallic silver. The synergetic effect was attributed to a cooperative mechanism in which Ag^{2+} oxidised CO, whereas the rapid reoxidation of Ag was ensured by oxygen transfer from Mn_2O_3, eliminating the slow process of Ag oxidation.

Silver appears incorporated in a mixed Ag–Mn oxide structure and stabilised in an oxidised form, since the catalyst is stable under oxygen up to 700 °C, whereas bulk AgO decomposes below 400 °C. The 5%$AgMnO_x$ catalyst is also very stable during soot oxidation under oxygen, since there is apparently no modification of the Mn_2O_3 phase nor formation of metallic silver, as shown by in-situ XRD. The XRD data collection, however, is very slow compared to the soot ignition process, and in situ XRD cannot reveal transient structural modifications.

Soot oxidation experiments in the absence of oxygen reveal that the $AgMnO_x$ catalyst supplies lattice oxygen at low temperature to oxidize the soot, and can be stoichiometrically reduced with successive crystal structure modifications ($Mn_2O_3 \rightarrow Mn_3O_4 \rightarrow MnO$) depending on the temperature, as shown by in-situ XRD and DTA-TGA experiments. Manganese reduction in $AgMnO_x$ is evidenced at a temperature as low as 240 °C, which is also the temperature range at which soot oxidation begins. This reduction is clearly favoured by direct physical contact between the catalyst and the soot, since it is not observed in the absence of soot and takes place at much lower temperatures in tight contact than in loose contact. Moreover, this contact is maintained up to deep reduction of the oxide, as observed for ceria/soot systems using other analytical procedures [11–13]. The reduced $AgMnO_x$ catalyst is reoxidised rather easily, MnO oxidation into Mn_3O_4 starting at 150 °C. Oxidation of Mn_3O_4 into Mn_2O_3, however, requires a temperature >350 °C and total Mn reoxidation into Mn^{3+} is achieved at 550 °C, in agreement with published data on pure manganese oxides [33]. The presence of metallic silver does not appear to influence Mn oxidation, in contrast with the reduction, probably because the oxidation of metallic silver is itself more difficult that the oxidation of MnO [40]. These results suggest that bulk catalyst reduction should be avoided since the complete catalyst reoxidation might require a higher temperature than the standard Diesel exhaust temperature range. However, under realistic conditions the DPF regeneration proceeds in the presence of oxygen, and oxygen total depletion leading to bulk catalyst reduction is unlikely since gas phase oxygen readily substitutes the lattice oxygen provided to the soot.

It is interesting to compare the activity of $AgMnO_x$ with that of perovskite $LaMnO_3$, studied in many oxidation reactions including carbon combustion. Fino et al. [5] compared the catalytic combustion of soot over $LaMnO_3$ and $LaCrO_3$ perovskites, and related the superior activity of the chromite to the presence of suprafacial, weakly adsorbed oxygen species. $LaMnO_3$ displayed negligible oxygen desorption at low temperature and was the least active catalyst. It became active only at high temperatures at which the lattice (or "intrafacial") oxygen became mobile. The authors proposed that suprafacial oxygen species were responsible for the high activity of $LaCrO_3$.

These observations suggest that manganese bulk reduction in the $LaMnO_3$ structure is difficult, because the perovskite structure is very stable due to the presence of La^{3+} ions in a fixed oxidation state, that require Mn ions in the 3+ oxidation state in order to satisfy the structure electroneutrality (despite a certain degree of oxygen non-stoichiometry authorised by La vacancies) [41]. In contrast, the reduction of $AgMnO_x$ by the soot is easy and related to the low temperature performances. In absence of gaseous oxygen, oxygen species desorb thermally from the catalyst in the 470–650 °C temperature range (Fig. 2B), whereas lattice oxygen starts to be transferred to the soot from 350 °C in tight contact (Fig. 5B). This suggests that there is no correlation between the activation energy of desorption/decomposition of oxygen from the catalyst and that of the diffusion process of active oxygen species from the catalyst to the soot via their physical contacts, in keeping with the conclusions of our previous experimental micro-kinetic studies on ceria [11,12].

4.2. Role of silver and mechanism of soot oxidation over $AgMnO_x$

Isotopic oxygen exchange experiments at 300 and 400 °C reveal a very limited exchange between lattice and gas phase oxygen, with only transient production of $^{18}O^{16}O$ in trace amount. Single atom exchange through dissociative oxygen adsorption (R^1-mechanism [42]) is clearly not favoured over the oxidised catalyst. Driscoll and Ozkan [43] reported a similar behaviour for the mixed oxide $MnMoO_4$. However, a slow, non-dissociative adsorption of molecular oxygen leading to a double exchange with lattice oxygen (R^2-mechanism) cannot be excluded.

The lack of oxygen exchange is consistent with the soot combustion experiment under $^{18}O_2$ evidencing the preferential incorporation of unlabelled oxygen in the oxidation products. After catalyst equilibration under $^{18}O_2$ for 10 min before the light-off, the lattice oxygen has essentially not been exchanged when the soot ignition begins. The soot ignition in tight contact mode appears initiated by the transfer of lattice oxygen from MnO_x to the soot (Mars and van Krevelen-type mechanism), this process being promoted by silver. This oxygen transfer leads to a rapid and transient catalyst reduction, probably restricted to the soot/catalyst interface. Once transferred to the soot, the lattice oxygen is rapidly replenished by $^{18}O_2$, as shown by the $^{18}O_2$ consumption starting simultaneously with CO_2 formation (Fig. 10A and C), which confirms that O_2 readsorption is not a limiting step during the soot oxidation. The diffusion of O^{2-} ions into the lattice might be the rate-limiting step of the reaction, since the formation of labelled CO_2 species becomes predominant only when the $C^{16}O_2$ signal has strongly fallen off. Since oxygen exchange is ineffective on the fully oxidised catalyst, the gaseous oxygen uptake might be driven by the formation of reduced sites, either Mn^{2+} or more likely metallic silver, as suggested by the transient formation of $^{18}O^{16}O$ and $^{16}O_2$ during soot combustion (Fig. 10C). The redox mechanism explains why after hydrothermal thermal ageing, which induces a 37% decrease in the surface area, the soot ignition temperature of aged $AgMnO_x$ is not modified compared to the fresh catalyst: adsorbed surface oxygen species do not contribute significantly to soot ignition at low temperature, in contrast to perovskite-type oxide catalysts [5,6]. Moreover, a moderate decrease in the BET surface area has a very limited impact on the amount and nature of the catalyst/soot contacts, particularly for the tight contact. The redox mechanism also explains the reduced catalyst performance under loose contact conditions, which is not related to a different mechanism but to a lower number of contacts.

The synergetic effect between silver and manganese appears related to the promotion of Mn^{3+} reducibility by silver, which also improves the incorporation of gas phase oxygen in the solid lattice and Mn^{2+} reoxidation.

5. Conclusion

We have studied the structural and redox properties of a 3.5%$AgMnO_x$ mixed oxide catalyst for Diesel soot combustion using in situ experiments. The catalyst was found very active at low temperature (<300 °C in tight contact), and the performances were not impaired after hydrothermal ageing at 750 °C. In situ XRD and DTA-TGA measurements showed that the catalyst was not modified during soot combustion experiments under oxygen, but under anaerobic conditions the soot was stoichiometrically oxidised by lattice oxygen through catalyst bulk reduction.

No significant exchange was observed between lattice oxygen and gaseous $^{18}O_2$, whereas soot oxidation experiments performed under $^{18}O_2$ revealed the preferential formation of unlabelled CO_2 and CO, evidencing a redox mechanism in which the soot ignition is initiated by the transfer of lattice oxygen from the catalyst to the soot through physical contacts. Adsorbed oxygen species do not appear to contribute significantly to the soot oxidation process.

A synergetic effect between silver and manganese appears responsible for the low temperature soot combustion activity, in which silver promotes the manganese oxide reducibility and the gas phase oxygen incorporation in the catalyst lattice.

Acknowledgements

The financial supports provided by RENAULT S.A. and ADEME are gratefully acknowledged. The authors thank N.S. Prakash for XPS measurements and data analysis.

References

[1] B.A.A.L. van Setten, M. Makkee, J.A. Moulijn, Catal. Rev. 43 (2001) 489.
[2] K.S. Martirosyan, K. Chen, D. Luss, Chem. Eng. Sci. 65 (2010) 42.
[3] J.A. Moulijn, F. Kapteijn, Carbon 33 (1995) 1155.
[4] D.W. McKee, J. Catal. 108 (1987) 480.
[5] D. Fino, N. Russo, G. Saracco, V. Specchia, J. Catal. 217 (2003) 367.
[6] N. Russo, D. Fino, G. Saracco, V. Specchia, J. Catal. 229 (2005) 459.
[7] G. Mul, F. Kapteijn, C. Doornkamp, J.A. Moulijn, J. Catal. 179 (1998) 258.
[8] M. Machida, Y. Murata, K. Kishikawa, D. Zhang, K. Ikeue, Chem. Mater. 20 (2008) 4489.
[9] A. Bueno-López, K. Krishna, M. Makkee, J.A. Moulijn, J. Catal. 230 (2005) 237.
[10] K. Shimizu, H. Kawachi, A. Satsuma, Appl. Catal. B 96 (2010) 169.
[11] B. Bassou, N. Guilhaume, K. Lombaert, C. Mirodatos, D. Bianchi, Energy Fuels 24 (2010) 4766.
[12] B. Bassou, N. Guilhaume, K. Lombaert, C. Mirodatos, D. Bianchi, Energy Fuels 24 (2010) 4781.
[13] S.B. Simonsen, S. Dahl, E. Johnson, S. Helveg, J. Catal. 255 (2008) 1.
[14] K. Yamazaki, T. Kayama, F. Dong, H. Shinjoh, J. Catal. 282 (2011) 289.
[15] E.E. Iojoiu, B. Bassou, N. Guilhaume, D. Farrusseng, A. Desmartin-Chomel, K. Lombaert, D. Bianchi, C. Mirodatos, Catal. Today 137 (2008) 103.
[16] B. Bassou, N. Guilhaume, E.E. Iojoiu, D. Farrusseng, K. Lombaert, D. Bianchi, C. Mirodatos, Catal. Today 159 (2011) 138.
[17] K. Lombaert, N. Moral-Mouaddib, N., Guilhaume, B., Bassou, E.E., Iojoiu, D., Bianchi, C. Mirodatos, Patent FR 2 939 328-A3 (2008).
[18] B. Bassou, N., Guilhaume, A. Desmartin-Chomel, D., Farrusseng, K., Lombaert, D., Bianchi, C. Mirodatos, unpublished results.
[19] K. Villani, R. Brosius, J.A. Martens, J. Catal. 236 (2005) 172.
[20] R. López-Fonseca, U. Elizundia, I. landa, M.A. Guttiérrez-Ortiz, J.R. González-Velasco, Appl. Catal. B 61 (2005) 150.
[21] B.R. Stanmore, J.F. Brilhac, P. Gilot, Carbon 39 (2001) 2247.
[22] B.A.A.L. van Setten, J.M. Schouten, M. Makkee, J.A. Moulijn, Appl. Catal. B 28 (2000) 253.
[23] CRC Handbook of Chemistry and Physics, 69th Edition (1988–1989).
[24] G.I.N. Waterhouse, G.A. Bowmaker, J.B. Metson, Phys. Chem. Chem. Phys. 3 (2001) 3838.
[25] J.F. Moulder, W.F. Stickle, P.E. Sobol, K.D. Bomben, in: J. Chaslain (Ed.), Handbook of X-ray Photoelectron Spectroscopy, PerkinElmer Corporation, 1992.
[26] G.I.N. Waterhouse, G.A. Bowmaker, J.B. Metson, Appl. Surf. Sci. 183 (2001) 191.
[27] W.-L. Dai, Y. Cao, L.-P. Ren, X.-L. Yang, J.-H. Xu, H.-X. Li, H.-Y. He, K.-N. Fan, J. Catal. 228 (2004) 80.
[28] F. Kapteijn, L. Singoredjo, A. Andreini, J.A. Moulijn, Appl. Catal. B: Environ. 3 (1994) 173.
[29] A. Williams, G.A. Butler, J. Hammonds, J. Catal. 24 (1972) 352.
[30] M. Pijolat, M. Dauzat, M. Soustelle, Solid State Ionics 50 (1992) 31.
[31] M.A. Villa Garcia, M.C. Trobajo Fernandez, C. Otero Arean, Thermochim. Acta 126 (1988) 33.
[32] F. Kapteijn, A.D. van Langeveld, J.A. Moulijn, A. Andreïni, M.A. Vuurman, A.M. Turek, J.-M. Jehng, I.E. Wachs, J. Catal. 150 (1994) 94.
[33] E.R. Stobbe, B.A. de Boer, J.W. Geus, Catal. Today 47 (1999) 161.
[34] M. Ferrandon, J. Carnö, S. Järås, E. Björnbom, Appl. Catal. A: Gen. 180 (1999) 141.
[35] A. Sadezky, H. Muckenhuber, H. Grothe, R. Niessner, U. Pöschl, Carbon 43 (2005) 1731.
[36] M. Che, A.J. Tench, Adv. Catal. 31 (1982) 77.
[37] M. Che, A.J. Tench, Adv. Catal. 32 (1983) 1.
[38] P.J. Gellings, H.J.M. Bouwmeester, Catal. Today 58 (2000) 1.
[39] M. Kobayashi, H. Kobayashi, J. Catal. 27 (1972) 100.
[40] S. Imamura, H. Sawada, K. Uemura, S. Ishida, J. Catal. 109 (1988) 198.
[41] L.G. Tejuca, J.L.G. Fierro, Adv. Catal. 36 (1989) 237.
[42] C. Doornkamp, M. Clement, V. Ponec, J. Catal. 182 (1999) 390.
[43] S.A. Driscoll, U.S. Ozkan, J. Phys. Chem. 97 (1993) 11524.